PHYSICAL REVIEW A **83**, 031802(R) (2011)

Digital reverse propagation in focusing Kerr media

Alexandre Goy and Demetri Psaltis
Laboratoire d'Optique, School of Engineering, École Polytechnique Fédérale de Lausanne, Switzerland
(Received 30 October 2010; published 9 March 2011)

Lenses allow the formation of clear images in homogeneous linear media. Holography is an alternative imaging method, but its use is limited to cases in which it provides an advantage, such as three-dimensional imaging. In nonlinear media, lenses no longer work. The light produces intensity-dependent aberrations. The reverse propagation method used in digital holography to form images from recorded holograms works even in Kerr media [M. Tsang, D. Psaltis, and F. G. Omenetto, Opt. Lett. **28**, 1873 (2003).]. The principle has been experimentally demonstrated recently in defocusing media [C. Barsi, W.Wan, and J.W. Fleischer, Nat. Photonics **3**, 211 (2009).]. Here, we report experimental results in focusing media.

DOI: 10.1103/PhysRevA.83.031802 PACS number(s): 42.65.−k, 42.40.−i

Focusing optical Kerr media have been widely studied since the discovery of self-focusing in the early sixties [1–3]. The attention of researchers was focused on the rich variety of physical phenomena that occur when intense light propagates through these media, but did not focus on imaging until recently [4]. Imaging through Kerr media has had no practical applications, but the increasing use of intense laser beams in applications such as microscopy, lithography, or micro-machining will likely require the development of nonlinear optical imaging technology. As opposed to imaging in defocusing media, imaging in focusing media is challenging because initial modulations may lead to filaments when the power exceeds the critical power for self-focusing, first introduced in [3,5]. We use the following definition: $P_{cr} = \pi 0.61^2 \lambda_0^2/(8 n_0 n_2)$, where λ_0 is the free-space wavelength, n_0 the refractive index, and n_2 [m^2/W] the nonlinear coefficient.

We investigate a classic imaging system in which a cell filled with acetone (the focusing nonlinear medium) is placed at the focal plane. At low intensity a high-quality image is produced, whereas at increasing intensities the interaction of the focused beam with the nonlinear medium results in a distorted image. The main result of this paper is the experimental demonstration of image formation in the presence of this strong focusing nonlinearity. We demonstrate that, with the proper choice of nonlinear index modulation and nonlinear absorption, very high quality images are produced by digital reverse propagation (DRP), which concept was first demonstrated in the time domain for fibers [6]. In our experiments, the power was gradually increased from the linear regime up to P_{cr}. In this way, we primarily characterize the nonlinear effects that are observed before strong self-focusing and filamentation takes place. A contrast inversion due to the nonlinearity [7–11] occurs at one-half the critical power. Close to and above this power, filamentation can occur, which generally makes the object reconstruction impossible. The fact that contrast inversion occurs at a given fraction of P_{cr} suggests that DRP can be used for the characterization of the nonlinear properties of the focusing media as an alternative to the Z-scan method [12].

The main approach for dealing with nonlinear aberrations is based on the time-reversal property of Maxwell equations to implement various kinds of phase conjugation (PC) [13–20]. Phase conjugation, however, produces an image at or near the object location, which is not accessible in most applications, and therefore its practical utility has been limited. Closely related to the phase conjugation principle, the DRP concept allows us to see through media involving a nonlinear process for which we have a proper physical model (see Fig. 1). The first application, as far as we know, of DRP in the spatial domain was the demonstration in defocusing photorefractive media [4].

In related work on the manipulation of spatial information in nonlinear media, it has been suggested that the nonlinear coupling between high and low spatial frequency modes can increase spatial resolution [4]. The nonlinearity can also be used to reveal weak signals in noisy environments by exploiting stochastic resonance [21], or simply to prevent diffraction blur through the use of spatial solitons as the sampling element [22].

As a physical model for digital propagation, we use the nonlinear Schrödinger equation (NLSE) based on Kerr nonlinearity. For continuous-wave monochromatic radiation, we have

$$\frac{\partial A}{\partial z} = \frac{i}{2k}\Delta_\perp A + i k_0 \tilde{n}_2 |A|^2 A - \frac{\beta n_0}{4\eta_0}|A|^2 A, \qquad (1)$$

where A (V/m) is the complex envelope of the field, z (m) is the propagation direction coordinate, $\Delta_\perp$ is the transverse Laplacian operator, n_0 is the linear refractive index, k_0 (m^{-1}) = $2\pi/\lambda$, $k = n_0 k_0$, $\tilde{n}_2$ (m^2/V^2) is the nonlinear coefficient, and β (m/W) is a nonlinear loss term defined by the drop of intensity: $I_z = -\beta I^2$, with $I = n_0|A|^2/2\eta_0$, with $\eta_0 = 377\Omega$. Note that n_2 (m^2/W) = $(2\eta_0/n_0)\tilde{n}_2$ (m^2/V^2). Equation (1) accounts for diffraction, self-phase modulation (SPM), and effective two-photon absorption. We use the split-step Fourier (SSF) beam propagation method (BPM) [23] to numerically evaluate Eq. (1).

The experimental setup is depicted in Fig. 2, the physical dimensions are provided in the supplementary material [24]. The acetone used as the nonlinear medium in the experiments has n_2 coefficient 3.6×10^{-21} m^2/W. This was measured by the Z-scan method for our particular laser pulse [24]. The laser source is a Ti:sapphire amplifier emitting 150-fs pulses centered at 800 nm, with 10-Hz repetition rate. The maximum energy per pulse is 2 mJ, and the best energy stability from pulse to pulse is ±2%. For these parameters, $P_{cr} = 19$ MW and we define the critical energy per pulse $E_{cr} = P_{cr}T = 2.9$ μJ,

 ©2011 American Physical Society

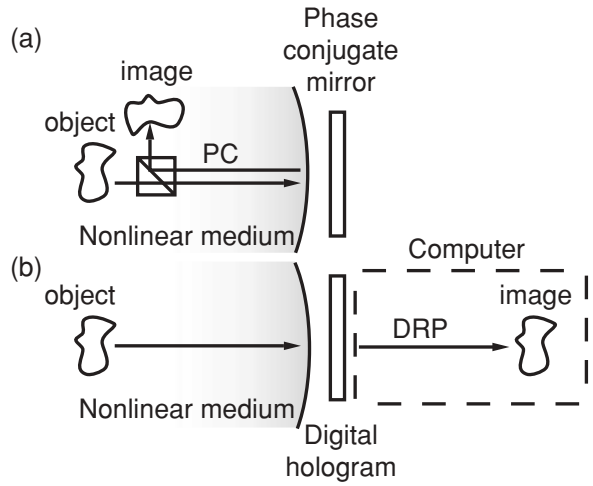

FIG. 1. Conceptual and practical differences between phase conjugation and DRP. Phase conjugation (a) does not require us to know the properties of the medium, but the image is formed at the object place. The beam splitter (BS) required to separate the image from the object would be on the wrong side of the medium. Conversely, for DRP (b), we need a model for the medium but the image is available in the computer.

where T is the pulse duration. The object consists of a chromium-coated glass U.S. Air Force resolution chart with dark patterns on a clear background, illuminated with convergent light, which focuses at the center of a 10-mm-thick acetone cell. The object itself is imaged onto the camera (CCD) with lenses located after the nonlinear medium. At low intensity we obtain a sharp image of the object. In order to reconstruct the object when the nonlinearity distorts its image, we record the full complex field on the CCD. For this purpose, we use off-axis holography to record amplitude and phase in a single shot. The pulse energy is measured independently with a photodiode.

This type of system is known to produce a contrast inversion of the object as already shown for thin nonlinear media placed at the focus of a lens [7–11]. The contrast inversion happens when the low spatial frequencies of the field carry most of the power and are nonlinearly phase shifted with respect to higher spatial frequencies. A digital model of the nonlinear imaging system shown on Fig. 2 was implemented in order to use reverse propagation. Lenses were represented by quadratic

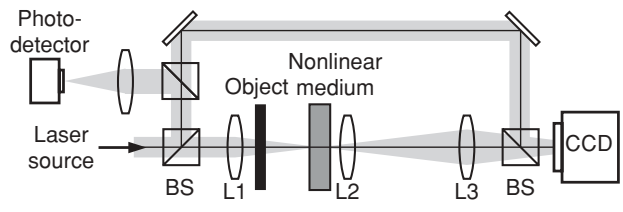

FIG. 2. Experimental setup. The object is illuminated with converging light focused by lens 1. The nonlinear medium is 10 mm thick and is centered about the focus. Lenses 2 and 3 produce an image of the object on the CCD. A reference beam is used to record the phase via off-axis holography. The delay line allows overlap of the signal and reference pulses. A photodetector is used to measure the actual pulse energy. For more details, see [24].

phase terms, free-space propagation was computed with single linear step of the BPM and nonlinear propagation in acetone with nonlinear SSF-BPM.

Figure 3 summarizes the results of three experiments done at increasing pulse intensities (0.87, 1.61,and 2.64 μJ, respectively, equal to $0.3E_{cr}$, $0.6E_{cr}$, and $0.9E_{cr}$). As expected, the reverse propagation properly undoes the effect of SPM and restores the object's original contrast (dark pattern on bright background) for pulse energies up to 0.8. We also include the result for an approximate Zernike filter that will be discussed later. As the energy comes closer to E_{cr}, an SPM-only model fails to provide the correct contrast. It has been observed that the low frequencies of the field are not only shifted but also undergo nonlinear absorption process.

When the total power becomes larger than P_{cr}, a filament is created at the focus and produces a colorful conical emission attributed to supercontinuum generation and four-wave mixing [25]. In our imaging system, this emission constitutes an effective loss mechanism. We show that the addition of the nonlinear gain term in Eq. (1) can effectively account for the loss. The empirical values of β that yielded the best reconstruction are $\beta = 8 \times 10^{-15}$ up to 2.2 μJ, $\beta = 10^{-14}$ m/W at 2.64 μJ, and $\beta = 1.6 \times 10^{-14}$ m/W at 2.8 μJ. The result is shown on Fig. 3(f) where the original contrast is successfully restored by the use of both SPM and gain in the reverse propagation. More information on the measurement of nonlinear absorption and its intensity dependence is provided in [24].

The nonlinearity in the systems of Fig. 2 is highly localized near the focal plane inside the acetone cell. Therefore we

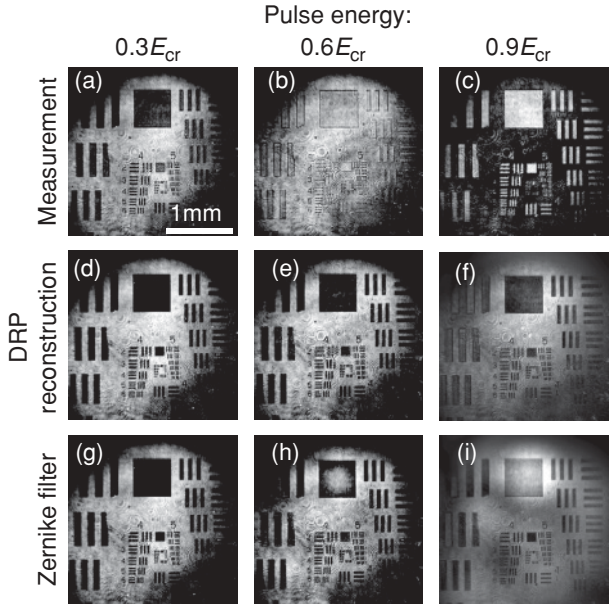

FIG. 3. Compared results of DRP and Zernike filter reconstruction. (a) to (c) Amplitudes of the measured output field recorded with the mentioned pulse energies. Note that linear reconstructions are similar except for a magnification factor. (d) to (f) Reconstruction of fields (a) to (c), respectively, using DRP. Both SPM and nonlinear gain are necessary to get a correct reconstruction in (f). (g) to (i) Zernike filters applied to measured field (a) to (c), respectively, with the following parameters: (g) $\phi = -\pi/5$, $g = 1$, (h) $\phi = -2\pi/5$, $g = 1$, and (i) $\phi = -5\pi/8$, $g = 3$. $k_c = 2\pi/1.4$ mm in all cases.

can approximate the nonlinear medium as a thin transparency whose amplitude and phase are modified by the presence of the light beam. The contrast inversion process can then be understood simply as a dynamic Zernike filter [26] automatically induced by the light beam itself. Accordingly the operation performed by reverse propagation can be approximated by a linear Zernike filter with the following transfer function: $T = \exp\{i W_{kc}[\phi - i \ln(g)]\}$, where W_{kc} is the circular window normalized to 1 with radius k_c centered about the origin in the Fourier domain. ϕ is a constant phase, and g is a constant gain ($\phi = \pi/2$ and $g = 1$ for the normal Zernike filter). Note that ϕ, g, and k_c are independent on the field.

The Zernike filter inversion method can be thought of as an alternative to DRP for inverting the nonlinear aberrations. However, at high power, the thin transparency approximation is less accurate for the nonlinear phase and intensity modulation of the light beam since the three-dimensional nature of the nonlinear medium becomes important at higher intensities. This effect is shown in the third row of Fig. 3 where the results of DRP and the Zernike approximation are compared. At a pulse energy of 2.64 μJ, DRP shows clearly a much sharper image reconstruction. Note that for the Zernike filter, the parameters k_c, ϕ, and g need to be determined through an exhaustive search or another search algorithm, whereas DRP only requires the knowledge of one parameter: the correct laser pulse energy.

The above results can be quantified by comparing the reconstruction provided by the reverse propagation and linear imaging (equivalent to linear reverse propagation). The distance between the two (complex) images X and Y is measured with a correlation coefficient r. X and Y are first normalized in order to have the same background as the lowest contrast image R. Then, we define $x = |X| - |R|$, $y = |Y| - |R|$, and

$$r(x,y) = \sum \frac{(x - \bar{x})(y - \bar{y})}{\sqrt{\sum (x - \bar{x})^2}\sqrt{\sum (y - \bar{y})^2}}, \qquad (2)$$

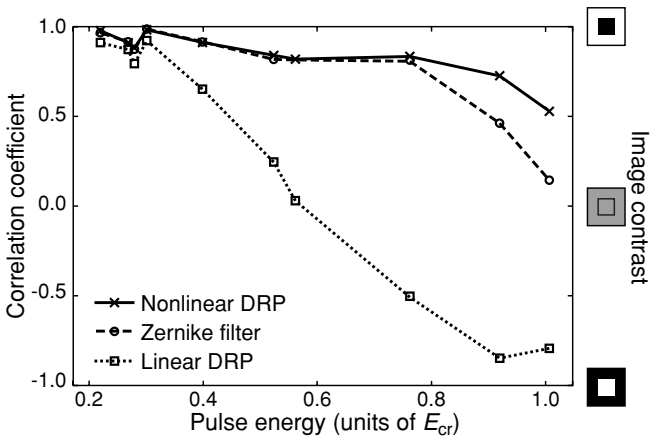

FIG. 4. Quantitative comparison between linear imaging, DRP, and Zernike filter. The correlation coefficient is computed between the current reconstruction and the low-intensity linear object, which is considered as a reference. The pulse energy is given in units of critical energy $E_{cr} = 2.9$ μJ (critical power times pulse duration). The value of the critical power is derived from the nonlinear coefficient n_2 measured by Z scan.

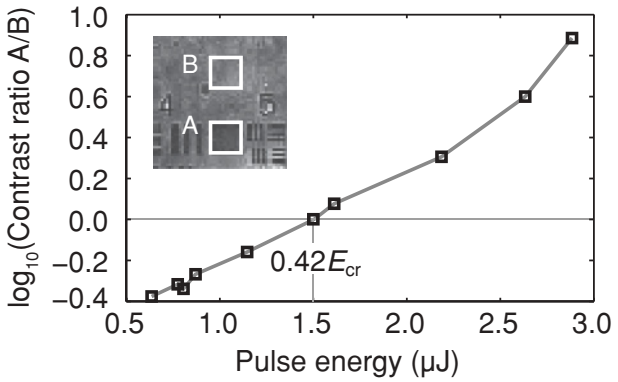

FIG. 5. Image contrast as a function of pulse energy. The contrast is quantified as the ratio of the integrated intensities in regions A and B. According to our empirical model, the curve crosses the contrast = 0 line at 0.424 times the critical energy E_{cr}. The value measured by Z scan is slightly lower, $0.424E_{cr} = 1.2$ μJ.

where the overbar denotes the average. With this definition, we get $0 < r < 1$ for the original contrast images, $r \approx 0$ for low contrast images, and $-1 < r < 0$ for inverted contrast images.

As shown on Fig. 4, the nonlinear reconstruction shows higher correlation with the object than the linear reconstruction, mainly because the latter fails to provide the correct contrast. At high energy, the DRP deteriorates because the loss in the low spatial frequency components is not completely compensated by the two-photon absorption term used to account for it (see [24] for a measurement of the absorption coefficient as a function of intensity). The conical emission associated with this loss also involves the generation of new frequencies that are neither accounted for in the model nor recorded by the hologram. The Zernike model is inferior (which compensates for the effects of nonlinear propagation with a two-dimensional transparency) to the DRP at high powers because the nonlinearity throughout the three-dimensional medium becomes more pronounced.

An important characteristic of reverse propagation through nonlinear media is that the nonlinear coefficient n_2 of the material has to be known. Conversely, if the pulse power is known accurately from experimental measurement, then n_2 can be determined by scanning its value until the reconstruction best matches the object. In this regard the contrast inversion setup can be an effective tool, since the contrast can be measured easily and the inversion occurs at a precise power.

The nonlinear coefficient n_2 is inversely proportional to the critical power for self-focusing which can in turn be related to the power P_{inv} at which the contrast inversion occurs. If the object is illuminated with a convergent Gaussian beam, then to each spatial frequency will correspond a focused beam with its waist in the Fourier plane. For transparent or reflective objects, the low spatial frequency components of the field are the strongest and we can assume that all the nonlinear phase shift occurs in the Gaussian beam corresponding to the zero frequency. This is equivalent to a Zernike filter, for which it is known that the minimum contrast image is obtained with a $\pm\pi/2$ phase shift.

We can derive a simple relationship to link the nonlinear phase shift of a Gaussian beam to its total power P. When

fitted to a numerical simulation, it gives a simple empirical relationship, as a function of $p = P/P_{\rm cr}$, for the nonlinear phase shift accumulated between $z = z_1$ and $z = z_2$:

$$\Phi_{\rm NL}(z_1,z_2) = (p + p^3)\phi, \tag{3}$$

where $\phi = \arctan(z_2/z_0) - \arctan(z_1/z_0)$ happens to be the Gouy phase shift between z_1 and z_2, $z = 0$ being the waist position, and z_0 the Rayleigh range of the beam. This model is valid when $|z_i|/z_0 > 1$. This allows us to predict the power at which we obtain a $\pi/2$ phase shift, corresponding to the lowest contrast image. If we require that $\int_{-\infty}^{\infty} \Phi_{\rm NL}(z)dz = \pi/2$, then we get an expression for the beam power at which the contrast inversion takes place: $P_{\rm inv} = 0.424 P_{\rm cr}$.

In the experiments, the contrast inversion occurs at 1.5 μJ, which provides a value for the nonlinear coefficient: $n_2 = 2.8 \times 10^{-21}$ m^2/W (see Fig. 5). The value obtained from the Z-scan measurement was $n_2 = 3.6 \times 10^{-21}$ m^2/W.

In conclusion, we have presented experimental results of image reconstructions using DRP through a focusing Kerr medium. In the convergent light system we used, the nonlinearity has pronounced effects even below critical power. This includes nonlinear losses and SPM, which are both corrected by DRP. We have also shown that an alternative reconstruction algorithm, a properly defined Zernike filter in the digital domain, can also correct nonlinear aberrations. We have found that DRP is superior at stronger light intensities. Finally, we have suggested that imaging in nonlinear media in conjunction with reverse propagation offers a tool to rapidly measure the nonlinear coefficient n_2 without the need for implementing a Z-scan experiment.

We would like to thank our colleague K. Makris for rich and constructive discussions.

[1] G. A. Askar'yan, Soviet. Phys. JETP **15**, 1088 (1962).
[2] M. Hercher, J. Opt. Soc. Am. **54**, 563 (1964).
[3] R. Y. Chiao, E. Garmire, and C. H. Townes, Phys. Rev. Lett. **13**, 479 (1964).
[4] C. Barsi, W. Wan, and J. W. Fleischer, Nat. Photonics **3**, 211 (2009).
[5] P. L. Kelley, Phys. Rev. Lett. **15**, 1005 (1965).
[6] M. Tsang, D. Psaltis, and F. G. Omenetto, Opt. Lett. **28**, 1873 (2003).
[7] V. Y. Ivanov, V. P. Sivokon, and M. A. Vorontsov, J. Opt. Soc. Am. A **9**, 1515 (1992).
[8] J. Glückstad, Opt. Commun. **120**, 194 (1995).
[9] M. Castillo, D. S. de la Llave, and R. R. Garciá, Opt. Eng. **40**, 2367 (2001).
[10] K. Komorowska and A. Miniewicz, J. Appl. Phys. **92**, 5635 (2002).
[11] K. Sendhil, C. Vijayan, and M. P. Kothiyal, Opt. Commun. **251**, 292 (2005).
[12] M. Sheik-Bahae, A. A. Said, T.-H. Wei, D. J. Hagan, and E. W. V. Stryland, IEEE J. Quantum Electron. **26**, 760 (1990).
[13] E. N. Leith and J. Upatniek, J. Opt. Soc. Am. **56**, 523 (1966).
[14] H. Kogelnik and K. S. Pennington, J. Opt. Soc. Am. **58**, 273 (1968).
[15] A. Yariv, Appl. Phys. Lett. **28**, 88 (1975).
[16] A. Yariv, Opt. Commun. **21**, 49 (1977).
[17] R. A. Fisher, B. R. Suydam, and D. Yevick, Opt. Lett. **8**, 611 (1983).
[18] T. Ogasawara, M. Ohno, K. Karaki, K. Nishizawa, and A. Akiba, J. Opt. Soc. Am. B **13**, 2193 (1996).
[19] G. Goldfarb, M. G. Taylor, and G. Li, IEEE Photonics Technol. Lett. **20**, 1887 (2008).
[20] X. Li, X. Chen, G. Goldfarb, E. Mateo, I. Kim, F. Yaman, and G. Li, Opt. Express **16**, 880 (2008).
[21] D. Dylov and J. W. Fleischer, Nat. Photonics **4**, 323 (2010).
[22] A. Bramati, W. Chinaglia, S. Minardi, and P. D. Trapani, Opt. Lett. **26**, 1409 (2001).
[23] J. A. Fleck, J. R. Morris, and M. D. Feit, Appl. Phys. **10**, 129 (1976).
[24] See supplemental material at [http://link.aps.org/supplemental/10.1103/PhysRevA.83.031802] for details on the Z-scan and on the measurement of the nonlinear absorption in acetone.
[25] X. Ni, C. Wang, X. Liang, M. Al-Rubaiee, and R. R. Alfano, IEEE J. Sel. Top. Quantum Electron. **10**, 1229 (2004).
[26] F. Zernike, Physica **9**, 686 (1942).